Inorganica Chimica Acta, 136 (1987) 165–171

Metal Ion–FTS Nonapeptide Interactions. A Quantitative Study of Zinc(II)–Nonapeptide Complexes (Thymulin) under Physiological Conditions and Assessment of their Biological Significance

BRAHIM HACHT and GUY BERTHON*

INSERM U 305, Laboratoire de Chimie Bioinorganique, Université Paul Sabatier, 38 rue des Trente-Six Ponts, 31400 Toulouse, France

(Received December 26, 1986)

Abstract

The biological activity of thymulin, a recently discovered metallo–nonapeptide, has been shown to be essentially zinc dependent.

The present paper reports a quantitative investigation of the complex formation equilibria between zinc and the involved FTS nonapeptide under physiological conditions. Two species have been characterized, namely ML_2H_2 and $M_2L(OH)_3$, whose biological significance has subsequently been assessed on the basis of appropriate computer simulations referring to *in vitro* (cell culture medium) and *in vivo* (blood plasma) applications.

Introduction

From FTS to Thymulin

Initially isolated from pig serum [1], the FTS molecule (namely 'Facteur Thymique Sérique') was first shown to be a nonapeptide involved in extrathymic T cell differentiation [2]. Its amino acid sequence was determined

(Glu-Ala-Lys-Ser-Gln-Gly-Gly-Ser-Asn

and the synthetic hormone proved biologically active [3].

However, the later synthesis of peptide batches which were unexpectedly revealed to be inactive drew attention to the possible incorporation of a metal ion in the native hormone [4]. Although clearcut evidence of the presence of any metal in the latter is still lacking for practical reasons [4, 5], it has nevertheless been definitely established that zinc ions fully restore the biological activity of the synthetic hormone previously incubated with the Chelex 100 chelating agent. Among the series of sixteen metals investigated in the above mentioned study [5], only aluminium and gallium proved to be as active as zinc.

Given that (i) zinc naturally occurs in relatively high concentrations in mammals [6], (ii) zinc deficiency induces a thymic involution [7] associated with a decreased level of the native hormone [8, 9], (iii) the presence of zinc in thymic epithelial cells has been demonstrated by immunofluorescence [5], (iv) high zinc concentrations have been determined in biologically active synthetic hormone batches whereas other batches with low zinc concentrations proved inactive [5], it was logically inferred that the active form of the hormone actually consists of the product of the association of the FTS nonapeptide with zinc. Accordingly, the corresponding metallopeptide was named 'Thymulin' [5].

More recently, monoclonal antibodies have been shown to specifically recognize the nonapeptide molecule when complexed with zinc, but neither the free molecule nor its complexed forms with other metals, notably aluminium [10].

Zinc–FTS Nonapeptide Interactions

Following the discovery of the natural occurrence of zinc in the native hormone, which actually makes it biologically active [5], a series of physicochemical studies was devoted to the research of the nature of the metal–peptide association.

The only (pseudo) quantitative investigation recently carried out used a gel filtration technique [11]. Zinc was shown to bind the nonapeptide between pH 6.5 and 9. At pH 7.5, the average number of zinc ions bound per FTS molecule was found to lie around one. This overall coordination number suggested the formation of a complex of 1:1 metal to ligand stoichiometry, whose apparent logarithmic stability constant was assessed to be about 6.30.

These results were in line with the optimal biological activity previously observed for equal concentrations of zinc and nonapeptide in an *in vitro* rosette assay where zinc overall concentration was fixed at 10^{-6} mol dm^{-3}. In addition, it appeared from comparisons based on coordination of zinc with FTS nonapeptide analogs that the Asn 9 carboxylate group as well as the peptide bond between Gln 5 and

*Author to whom correspondence should be addressed.

0020-1693/87/$3.50

Gly 6 would be involved in the binding between zinc and the nonapeptide, but the exact localization of the metal coordination site could not be ascertained [11].

More recently, NMR determinations carried out in DMSO led to the conclusion that with the nonapeptide zinc forms a complex of 1:1 stoichiometry in which the ⟨Glu1-Ala2-Lys3 moiety is not involved, but which implies the participation of the terminal Asn carboxylate and of Ser 4 and 8 hydroxides in the metal coordination [12].

Nevertheless, the above two studies call for the following remarks:

(i) as was pointed out by the authors of the first one [11], their measurements reflect the influence of an overall phenomenon which may sum up more complex individual reactions;

(ii) as far as the second is concerned, its conclusions are relevant to DMSO, an organic solvent to which phospholipid cell membranes may be likened, but certainly not aqueous biofluids. This remark appears all the more valid since it has recently been shown that the conformation of the free nonapeptide varies to a very significant extent from DMSO to water [13].

Furthermore, both of these studies suggest the non interference of the ϵ-amino group of Lys 3 in zinc coordination, whereas the presence of this aminoacid residue was recognized to be absolutely necessary for biological activity [14]. On the other hand, as it is also well established that this activity is conferred on free nonapeptide by zinc ions, it would seem logical that these two requirements be interrelated.

Solving this problem requires further information on the formation of Zn–FTS nonapeptide complexes under experimental conditions closer to the physiological medium. The present paper thus reports a quantitative investigation of the corresponding equilibria in aqueous NaCl 0.15 mol dm^{-3} at 37 °C. Appropriate computer simulations of the distribution of each of both reactants *in vitro* and *in vivo* are then used to assess the biological significance of their predominant species.

Experimental

Formation Constant Determinations

Materials

The sample of synthetic nonapeptide used in these studies was supplied by Institut Choay, Paris, France. This sample proved to contain traces of non removable acetate, which were clearly characterized by NMR analysis. The nonapeptide content is given near 95% in weight as based on HPLC, aminoacid and elemental analysis. Account being taken of the relative values of acetate and nonapeptide molecular weights, the latter percentage corresponds to an almost equimolar stoichiometry of the two compounds. Accordingly, every fresh solution of this sample had to be analysed for both acetate and nonapeptide before use. This required the investigation of the acetate protonation equilibrium separately, which was done using Prolabo R.P. Normapur acetic acid.

The standard stock solution of zinc was prepared by dissolving crystals of its chloride salt (Merck pro analysi reagent) in diluted hydrochloric acid. It was titrated for its metal and proton contents as reported earlier [15].

Stock solutions of sodium hydroxide were prepared by diluting BDH ampoules in freshly boiled double deionized water and were maintained constantly under nitrogen. They were standardized and proved to be carbonate free as previously described [16].

Merck pro analysi sodium chloride 0.15 mol dm^{-3} was used as a background electrolyte to maintain activity coefficients constant and to ensure isotonicity with blood plasma.

Technique and equipment

On account of the small amount of synthetic nonapeptide available, potentiometric titrations were performed using a Metrohm E105 combined micro electrode, fitted in a thermostatted Metrohm 5 cm^3 cell unit. E.m.f. variations were monitored by a digital mV-meter Beckman model 4500.

The temperature of the reaction vessel was maintained at 37 ± 0.02 °C and all titrations were carried out under a constant bubbling of purified and thermostatted nitrogen.

Solutions of the nonapeptide sample to be titrated were made sufficiently acidic for all the dissociating groups of the two ligands (peptide and unremovable acetate) to be protonated at the outset of each experiment. Successive aliquots of sodium hydroxide 0.02 mol dm^{-3} were delivered from a Radiometer ABU 12 Autoburette equipped with a 2.5 cm^3 glass cylinder, both titrate and titrant containing NaCl 0.15 mol dm^{-3}.

Ligand–proton and metal–ligand ratios were varied significantly, as may be noted in Table I where titration data are summarized. Concerning the pH values appearing in this Table, two independent remarks are in order:

(i) it is logical that titrations be stopped whenever a steady drift is observed in the mV-meter readings, indicative of the appearance of a precipitate in the solution. Nevertheless, data collected beyond true equilibrium conditions may sometimes be useful in defining the stoichiometry of species predominating under such conditions [17]. Such a situation has been encountered in the Zn–nonapeptide system, for which a precipitate appeared in solutions of various

TABLE I. Summary of the Titration Data Used for These Studies[a]

System	C_{Zn}	C_{ac}	C_{FTS}	C_H	pH range
Proton–acetate		1.25			3.78–8.70
		2.50			3.63–7.15
		5.00			3.46–8.97
Zinc–acetate	2.54	5.00		0.27	3.30–6.98
	5.07	10.00		0.54	3.09–6.95
	10.15	30.00		1.08	2.81–7.03
	10.15	20.00		1.08	2.85–6.90
Proton–FTS		0.44	1.39	10.05	2.10–10.22
		0.47	1.18	5.02	2.47–10.32
		0.86	2.35	10.05	2.17–10.42
		0.45	1.18	2.51	2.90–10.41
		0.86	2.35	5.02	2.65–10.53
		1.31	3.56	8.04	2.47–10.58
		1.24	3.76	8.04	2.48–10.59
Zinc–FTS	1.02	1.24	3.76	8.11	2.44–6.94 [9.60]
	0.64	0.86	2.35	5.07	2.66–6.93 [9.50]
	1.02	0.86	2.35	5.09	2.61–6.99 [8.51]
	0.51	0.47	1.18	5.06	2.45–6.99 [7.31]
	2.54	0.86	2.35	5.21	2.60–7.02 [7.36]
	3.81	0.86	2.35	5.30	2.59–6.99 [7.23]
	2.29	0.47	1.18	5.18	2.46–7.31
	2.54	0.44	1.18	5.21	2.42–7.27

[a]Initial total concentrations of zinc (C_{Zn}), acetate (C_{ac}), FTS nonapeptide (C_{FTS}) and hydrochloric acid (C_H), and pH range *Chim. Acta, 125,* 219 (1986).

concentrations near pH 7. Some titrations were thus rapidly pursued beyond this limit in order to get a better idea of the nature of the presumably precipitated species. Whenever this has been done, the pH limit reached in the presence of the precipitate is given in brackets;

(ii) the above electrode system was calibrated in the concentration scale [18], and the ionic product of water was found to be $10^{-13.24}$ under the present conditions. Accordingly, the symbol pH used throughout actually represents –log [H].

Calculation procedures

Our classical approach [16, 19, 20] successively involving optimization and simulation steps was used to refine protonation and complex formation constants. However, on account of the undesired presence of an unknown amount of acetate in the nonapeptide sample, these calculations became more complicated than usual. In addition to the determination of proton– and zinc–nonapeptide equilibrium constants, we had also to determine the respective nonapeptide and acetate contents of the stock solutions simultaneously.

It was carried out in three stages:

(i) proton– and zinc–acetate equilibria were first investigated separately using the above mentioned approach [16, 19, 20], corresponding formation constants being held constant during subsequent calculations;

(ii) estimates of the nonapeptide protonation constants were initially derived from the shapes of mixed-ligand protonation curves representing the average number of protons bound to both nonapeptide (FTS) and acetate (ac) ligands as a function

$$\bar{r} = (C_H + C_{FTS} + C_{ac} - C_{OH} - [H] + [OH])/(C_{ac} + C_{FTS})$$

of pH, these curves being themselves approximate since they are based on estimated ligand concentrations.

Nonapeptide protonation constants were then refined together with both peptide and acetate concentrations using the ESTA optimization module [21], and new protonation curves were subsequently drawn on the basis of optimized ligand concentrations. The outcome of these calculations was confirmed by refining nonapeptide protonation constants once more by means of the MINIQUAD programme [22] fed with the optimized ligand concentrations.

Finally, mixed-ligand protonation curves were simulated by the appropriate module of the ESTA library [21] as they would have been experimentally obtained in the hypothesis of the above constants and concentrations.

TABLE II. Formation Constants Determined in These Studies[a]

System	p	q	r	$\log \beta$	S	R	n
Proton–acetate	1	0	1	4.526 ± 0.002	1.17E − 8	0.0034	84
Zinc–acetate	no complex in evidence under Table 1 conditions						
Proton–FTS	1	0	1	9.703 ± 0.002	1.02E − 7	0.0050	359
	1	0	2	12.929 ± 0.005			
Zinc–FTS	2	1	2	24.255 ± 0.066	2.67E − 7	0.0087	209
	1	2	−3	−14.176 ± 0.025			
	(0	1	−1	−8.378 ± 0.110)			

[a]The formula of the general complex is $M_qL_pH_r$. S = sum of squared residuals; R = R factor as defined in ref. 22; n = number of experimental observations.

Among these successive operations, those which are necessary to optimize ligand concentrations were repeated whenever a fresh solution of the nonapeptide sample was prepared. Nonapeptide protonation constants as well as concentrations of both ligands were then held constant in subsequent calculations;

(iii) once all parameters determined in stages (i) and (ii) attributed a fixed value, the investigation of Zn–peptide complex equilibria could then be envisaged. In the present case, it was impossible to employ our usual procedure pertinent to binary systems [16, 19]. In particular, the very useful notion of a complex formation curve [16, 19] becomes meaningless in the presence of two ligands. We thus had to use mixed-ligand protonation curves in the presence of a metal, a graphical medium normally specific to ternary systems [20]. Formation constants were refined with MINIQUAD [22], simulations being performed by means of the ESTA appropriate module [21].

All calculations were carried out at CICT (Toulouse) and CIRCE (CNRS, Orsay) computing centers through the EARN network.

Results and Discussion

The formation constants determined in these studies are shown in Table II.

Proton– and Zinc–Acetate Equilibria

As may be seen in Table II, no complex could be characterized between zinc and acetate under experimental conditions reported in Table I. Indeed, acetate protonation curves in the presence and absence of zinc were found to be exactly superimposable.

This does not preclude the existence of such complexes at far higher concentrations of acetate, but definitely rules out any possibility of them existing to a significant extent within the concentration range investigated. Since this range includes chosen values much greater than those which pertain to acetate-containing nonapeptide solutions, this suggests that zinc–acetate interactions will not interfere at all with zinc–nonapeptide ones, and thus can be safely neglected in corresponding calculations.

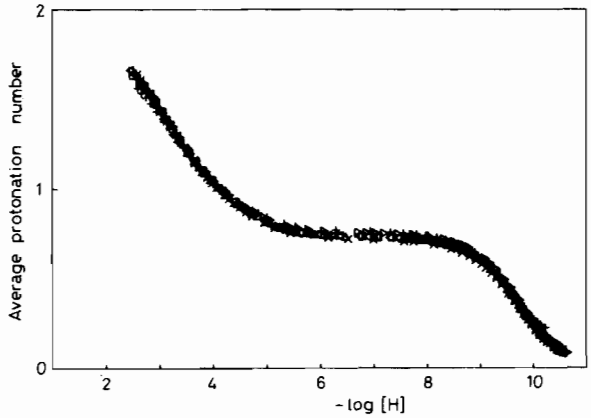

Fig. 1. Experimental protonation curves relative to the FTS nonapeptide–acetate mixture. The following symbols correspond to the respective order of the experiments summarized in Table I: +, x, □, △, ▽, ◁, ▷.

Proton–Nonapeptide Equilibria

Experimental protonation curves relative to the acetate containing nonapeptide solutions are shown in Fig. 1, as obtained from optimized concentrations of both ligands (see above). Their simulated homologues based on results in Table II are shown in Fig. 2. A quite satisfactory coincidence may be observed between these two Figures, which confirms the validity of the approach used.

Zinc–Nonapeptide Equilibria

Figure 3 shows the experimental mixed-ligand protonation curves relative to the various metal to ligand ratios investigated (Table I), with data limited to true equilibrium observations (see above). Compared to the same curves in the absence of metal

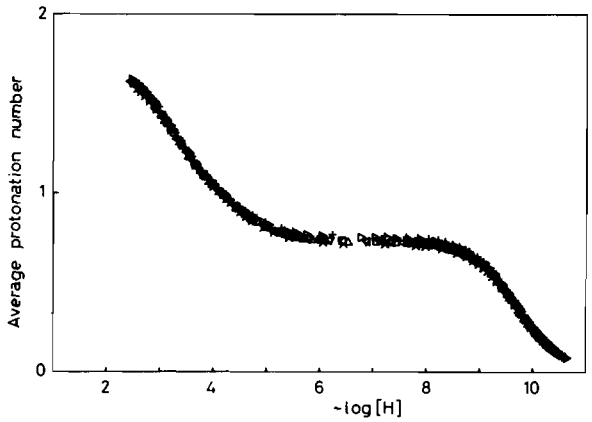

Fig. 2. Simulated protonation curves relative to the FTS nonapeptide–acetate mixture as obtained by means of the ESTA programme using results in Table II; key to symbols as in Fig. 1.

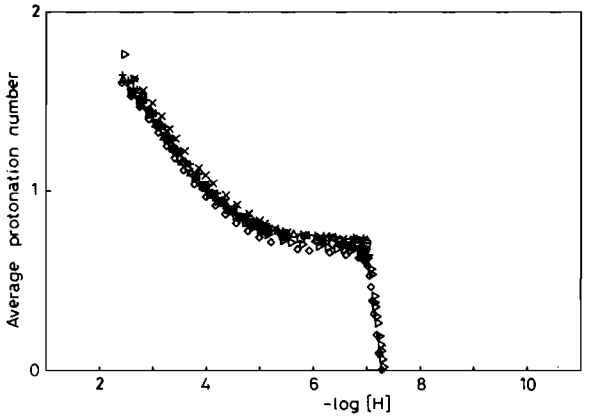

Fig. 3. Experimental protonation curves relative to the FTS nonapeptide–acetate mixture in the presence of various concentrations of zinc, limited to true equilibrium observations (see text). The following symbols correspond to the respective order of the experiments summarized in Table I: +, x, □, △, ▽, ◁, ▷, ◇.

(Fig. 1), the most striking difference is the drift of the most basic protonation step, which actually refers to the ϵ-amino group of Lys 3, towards more acidic pH values. The variable extent of this shift may be observed in more detail on the curves corresponding to the full pH range investigated (Fig. 4).

This effect, which appears to be metal-concentration dependent, may *a priori* be due either to the nonapeptide coordination by zinc or to zinc hydrolysis, since both phenomena would similarly result in an overall release of protons. The occurrence of a $Zn(OH)_2$-like precipitate near pH 7 would suggest the presence of this hydroxide in solution, but this does not preclude the possible formation of zinc-nonapeptide complexes simultaneously.

Research on the zinc–nonapeptide complexes was first carried out using data strictly referring to true equilibrium observations (Fig. 3). From a practical

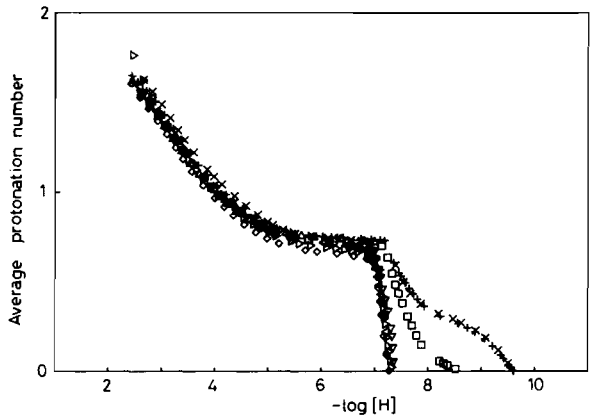

Fig. 4. Experimental protonation curves relative to the FTS nonapeptide–acetate mixture in the presence of various concentrations of zinc, over the full pH range investigated; key to symbols as in Fig. 3.

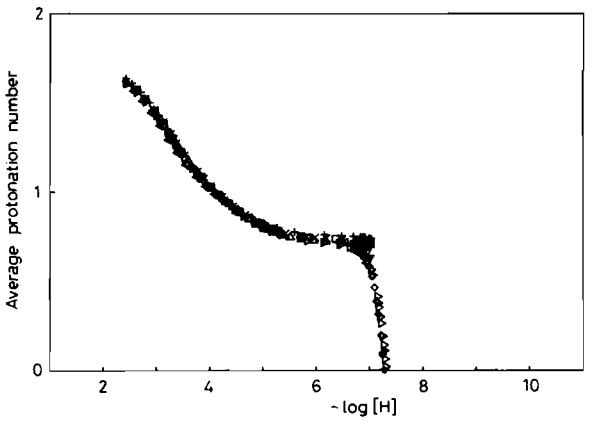

Fig. 5. Simulated protonation curves corresponding to the experimental data shown in Fig. 3, as obtained by means of the ESTA programme using results in Table II; key to symbols as in Fig. 3.

point of view, a large number of combinations of the following potential species were tested: MLH, ML_2H, ML_2H_2, M_2L, ML, ML_2, $M_2L(OH)$, $M_2L(OH)_2$, $M_2L(OH)_3$, $M_2L(OH)_4$, $ML(OH)$, $M_2L_2(OH)_2$, $ML_2(OH)$, $ML_2(OH)_2$, where L represents the anionic form of the peptide, M being given for zinc. Zinc hydroxide formation constants were considered in these calculations, with 4.21 and 9.48 logarithmic values for $Zn(OH)$ and $Zn(OH)_2$ respectively [23]. They were first held constant during refinements, then were finally allowed to vary with the 'best' set of species, which significantly improved numerical fits [17]. Among the above species, only those reported in Table II could be characterized under the present conditions. In particular, the ML species proved systematically insignificant in all combinations, whereas $M_2L(OH)_3$ was found to be absolutely necessary to simulate the experimental formation curves (Fig. 5).

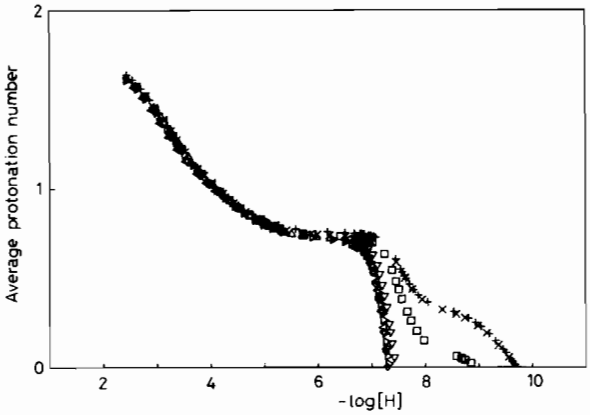

Fig. 6. Simulated protonation curves corresponding to the experimental data shown in Fig. 4, as obtained by means of the ESTA programme using the constants determined over the full pH range investigated (see text); key to symbols as in Fig. 3.

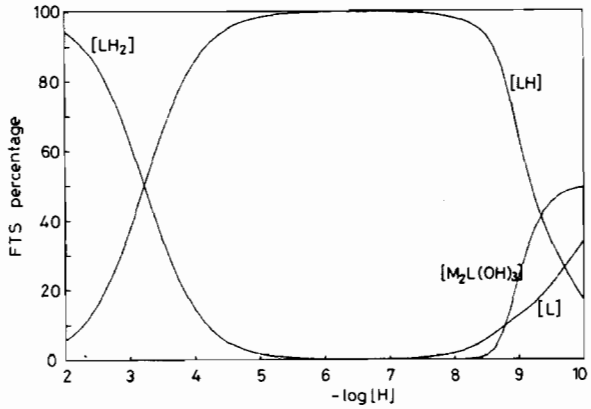

Fig. 7. Simulated distribution of the FTS nonapeptide into its free, protonated, and zinc-complexed species as a function of pH, with zinc and FTS concentrations equal to 10^{-6} mol dm^{-3}.

As outlined in a previous paragraph, this research was then extended to the full pH range investigated, in order to get more information on the nature of the species coexisting with the precipitate: the occurrence of $M_2L(OH)_3$ along with ML_2H_2 in solution was clearly confirmed with very similar constants, the only difference noted concerned zinc hydroxides. Indeed, instead of Zn(OH) whose constant was now made negative during refinement, $Zn(OH)_2$ was proved to exist to a significant extent. Moreover, the examination of the corresponding MINIQUAD output revealed that $Zn(OH)_2$ and $M_2L(OH)_3$ coexist in the pH precipitation range. This definitely confirms the existence of the above hydroxo species, and suggests that the precipitate does correspond to zinc dihydroxide. As a matter of fact, both $Zn(OH)_2$ and $M_2L(OH)_3$ proved necessary to simulate the experimental curves above pH 7 (Fig. 6).

Computer Simulation Studies

Objectives

It may be of interest to simulate the distribution of Zn–nonapeptide complexes under conditions specific to previous biological tests. This allows the assessment of which particular species is quantitatively predominant under these conditions, hence likely to represent the active form of the peptide. Such simulations were thus applied to zinc and nonapeptide concentrations recognized as optimal for exhibiting biological activity as far as the rosette assay is concerned. This was done using our plotting updated BASIC version of the COMICS programme [24].

Thymulin is now being used in clinical trials as a drug against rheumatoid arthritis. It may thus be of interest to get a quantitative knowledge of its interactions with zinc in blood plasma during treatment. Corresponding simulations were performed by means of the ECCLES programme [25], after incorporation of Table II constants into our current databank.

Results

Simulations Referring to Rosette Assay Conditions

Figure 7 shows the distribution of the nonapeptide into its free, protonated and zinc-complexed species as a function of pH.

Clearly, the influence of zinc–peptide interactions on the nonapeptide distribution remains quantitatively insignificant up to pH 8 for the concentrations under consideration (this is no longer the case for higher concentrations, as was established from other simulations not shown here). Since interactions with other reactants present in the culture medium used for the rosette assay [5] would rather tend to reduce the above concentrations, this influence should be considered as a maximum.

However, it should be borne in mind that the $M_2L(OH)_3$ species which becomes significant near pH 8 on Fig. 7 is electrically neutral, hence likely to penetrate cell membranes where it may initiate the thymulin action. In such a case, even a very low percentage of a given species may indeed be sufficient for it to be biologically active [26].

If the role played by thymulin was only due to the capacity of the nonapeptide to diffuse through cell membranes, its biological activity would probably be observed over the whole pH range investigated in Fig. 7; indeed, its (also electrically neutral) monoprotonated species is largely predominant throughout. The fact that this biological activity was shown to be optimal near pH 7–8.5 [5] suggests that the

$M_2L(OH)_3$ species is involved in a specific interaction between thymulin and cell membranes. Concerning this interaction, the question still remains as to whether it is due to the particular conformation that zinc confers on the nonapeptide through the above species, or to the formation of a zinc ternary complex with a second ligand inside the membrane.

Simulations Referring to Blood Plasma During Treatment of Rheumatoid Arthritis

Based on the dose of 5 mg/kg administered subcutaneously (P. Lefrancier, private communication), the average concentration of thymulin in blood plasma during treatment can be considered to lie around 8×10^{-5} mol dm^{-3}. The FTS nonapeptide concentration was thus scanned from 10^{-6} mol dm^{-3} to 10^{-2} mol dm^{-3}, which corresponds to realistic extreme limits.

As is often the case for plasma ligands [25, 27], and whatever its overall concentration may be, the nonapeptide occurs in plasma almost exclusively (99.5%) in the form of its neutral monoprotonated species LH, the remainder being represented by its free anion (0.5%). It thus seems that the diffusion of the nonapeptide into tissues would essentially be due to the overwhelming predominance of LH.

Zinc–nonapeptide complexes appear to exist in the form of MLXH ternary species, where L stands for the nonapeptide and X for each of the aminoacids occurring naturally in blood plasma. The sum of the concentrations of these complexes is 10^5 times lower than that of LH alone. In particular, the $M_2L(OH)_3$ species mentioned in the above paragraph is 2×10^{12} less concentrated than LH. This observation suggests that the active zinc–nonapeptide species *in vivo* may be different from that which conditions the activity of the peptide *in vitro*.

As for the potential effect of the nonapeptide on zinc distribution in plasma, simulations have shown that the fraction of low-molecular-weight zinc bound to it varies from 0.1% (for $C_{FTS} = 3 \times 10^{-5}$ mol dm^{-3}) to about 30% (for $C_{FTS} = 10^{-2}$ mol dm^{-3}). This effect, although not important at thymulin therapeutic concentrations, should not be considered as utterly negligible, the more so as the most predominant species, *i.e.* Zn–L–Cys–H, is electrically neutral and thus likely to diffuse into tissues.

Acknowledgements

The authors thank Prof. J. F. Bach (INSERM U25 and CNRS LA122, Hôpital Necker, Paris) for introducing them to the matter of this work, Dr. P. Lefrancier (Institut Choay, Paris) for his gift of the synthetic nonapeptide sample and for useful suggestions in the writing of the present paper, Dr. J. P. Laussac (LCC CNRS, Toulouse) for the NMR analysis of the above sample, and Dr. M. Dardenne for helpful discussions.

References

1 J. F. Bach and M. Dardenne, *Immunology, 25,* 353 (1973).
2 J. F Bach, M. Dardenne, J. M. Pleau and J. Rosa, *C. R. Acad. Sci., Sér. D, 283,* 1605 (1976).
3 J. F. Bach, M. Dardenne, J. M. Pleau and J. Rosa, *Nature (London), 266,* 55 (1977).
4 M. Dardenne, J. M. Pleau, P. Lefrancier and J. F. Bach, *C. R. Acad. Sci., Sér. III, 292,* 793 (1981).
5 M. Dardenne, J. M. Pleau, B. Nabarra, P. Lefrancier, M. Derrien, J. Choay and J. Bach, *Proc. Natl. Acad. Sci. U.S.A., 79,* 5370 (1982).
6 E. J. Underwood, 'Trace Elements in Human Health and Animal Nutrition', 4th edn., Academic Press, New York, 1977.
7 R. J. Chandra, in 'Immunology of Nutritional Disorders', Arnold, London, 1980, p. 49.
8 T. Iwata, G. S. Incefy, T. Tanaka, G. Fernandez, C. J. Menedez-Botet and R. A. Good, *Cell. Immunol., 47,* 100 (1979).
9 R. K. Chandra, G. Heresi and A. U. Bing, *Clin. Exp. Immunol., 42,* 332 (1980).
10 M. Dardenne, W. Savino, S. Berrih and J. F. Bach, *Proc. Natl. Acad. Sci. U.S.A., 82,* 7035 (1985).
11 L. N. Gastinel, M. Dardenne, J. M. Pleau and J. F. Bach, *Biochim. Biophys. Acta, 797,* 147 (1984).
12 J. P. Laussac, R. Haran, M. Dardenne, P. Lefrancier and J. F. Bach, *C. R. Acad. Sci., Sér. III, 301,* 471 (1985).
13 J. P. Laussac, M. T. Cung, M. Pasdeloup, R. Haran, M. Marraud, P. Lefrancier, M. Dardenne and J. F. Bach, *J. Biol. Chem., 261,* 7784 (1986).
14 J. F Bach, in 'Clinics in Immunology and Allergy', Vol. 3, Saunders, Philadelphia, 1983, pp. 133–156.
15 F. Akrivos, M. J. Blais, J. Hoffelt and G. Berthon, *Agents Actions, 15,* 649 (1984).
16 M. J. Blais and G. Berthon, *J. Chem. Soc., Dalton Trans.,* 1803 (1982).
17 M. Venturini and G. Berthon, *J. Chem. Soc., Dalton Trans.,* in press.
18 P. W. Linder, R. G. Torrington and D. R. Williams, 'Analysis Using Glass Electrodes', Open University Press, Milton Keynes, 1984.
19 G. Berthon, P. M. May and D. R. Williams, *J. Chem. Soc., Dalton Trans.,* 1433 (1978).
20 T. Alemdaroglu and G. Berthon, *Inorg. Chim. Acta, 56,* 115 (1981).
21 K. Murray and P. M. May, 'ESTA Users Manual', UWIST, Cardiff, 1984.
22 A. Sabatini, A. Vacca and P. Gans, *Talanta, 21,* 53 (1974).
23 L. G. Sillen and A. E. Martell, 'Stability Constants', Special Publication No. 17, The Chemical Society, London 1964, Suppl. No. 1; Special Publication No. 25, London 1971.
24 D. D. Perrin and I. G. Sayce, *Talanta, 14,* 833 (1967).
25 P. M. May, P. W. Linder and D. R. Williams, *J. Chem. Soc., Dalton Trans.,* 588 (1977).
26 G. Berthon, C. Blaquiere, A. Varsamidis and D. Rigal, *XXIV ICCC,* Athens, August 24–29, 1986.
27 G. Berthon, B. Hacht, M. J. Blais and P. M. May, *Inorg. Chim. Acta, 125,* 219 (1986).